KSCE Journal of Civil Engineering (2022) 26(5):2420-2427
DOI 10.1007/s12205-022-0401-1

pISSN 1226-7988, eISSN 1976-3808
www.springer.com/12205

Tunnel Engineering

Calculation of the Allowable Drainage of Parallel Tunnels Based on Ecological Environment Protection

Helin Fu[a,b], **Pengtao An**[a,b], **Guowen Cheng**[c], **Shujie Wen**[d], **and Jie Li**[a,b]

[a]*School of Civil Engineering, Central South University, Changsha 410075, China*
[b]*National Engineering Laboratory of High-Speed Railway Construction Technology, Central South University, Changsha 410075, China*
[c]*Guangdong Nanyue Transportation Investment and Construction Co., Ltd., Guangzhou 510101, China*
[d]*School of Civil and Surveying & Mapping Engineering, Jiangxi University of Science and Technology, Ganzhou 341000, China*

ARTICLE HISTORY

Received 10 March 2021
Revised 19 October 2021
Accepted 14 December 2021
Published Online 12 February 2022

KEYWORDS

Controlled drainage
Parallel tunnel
Steady flow
Falling funnel
Water storage coefficient

ABSTRACT

To determine a reasonable value of parallel tunnel drainage, a steady-flow calculation model is established. The differential equilibrium equation of seepage is established, and the equation of the falling funnel curve in a steady state with drainage parameters is solved by using boundary conditions. The maximum drawdown depth of the control point is used to calculate the allowable discharge of the tunnel. Then, the curve equation of the falling funnel is determined, the volume of the drainage funnel is calculated, and the total discharge in the steady state is calculated according to the water storage coefficient. Finally, the theoretical formula is verified based on an engineering case and numerical simulation. Considering the actual engineering geology and hydrogeological conditions of the tunnel site, the total drainage, allowable drainage, and initial support bearing head height calculated with the proposed method are different from the actual measurements collected on site by 10%, 18.9% and 13.6%, respectively. Therefore, the calculation method can provide a reference for similar engineering.

1. Introduction

For tunnels rich in groundwater, if the design or construction is unreasonable, groundwater will continuously flow into the tunnel during the whole construction process and operation period, which which will worsen the ecological environment or cause frequent water damage in tunnels, affect the traffic safety of tunnels, and reduce the durability of the lining structures (Gokdemir et al., 2019; Cheng et al., 2020). Comprehensively considering the ecological environment and structural safety factors, the design criteria of water control and drainage in the high-water level area are mostly "plugging and limited discharge", i.e., "water plugging and limited discharge" (Sembenelli and Sembenelli, 1999; Tao et al., 2015; Cheng et al., 2019a). However, the research on water inrush disaster treatment and allowable water inflow prediction has not established a relatively perfect theoretical system, and the research methods are mostly based on experience (Nilsen, 2014; Li and Mo, 2020; Fu et al., 2022). The allowable seepage into the tunnel is mostly based on experience.

With the help of underground hydraulic theory and seepage differential equation, Li et al. (2017), Zhang and Sun (2019), Park et al. (2008) and Kolymbas and Wagner (2007) assumed that no water pressure acts on the inner wall of a supporting structure and analysed the seepage field near the tunnel and the influencing factors of the seepage flow, providing theoretical guidance for the design of the grouting reinforced region. Cheng et al. (2019b) established a groundwater seepage model. Due to the model and groundwater dynamics, the relationship between the amount of water inflow and drawdown of the groundwater table for a tunnel is derived under unsteady flow conditions. Yang et al. (2009) used the Groundwater Modeling System (GMS), which is a groundwater modelling software package that supports the groundwater digital codes MODFLOW and FEMWATER, to determine the impact of tunnel excavation on the hydrogeological environment of the area around the tunnel. By using a laboratory model test, Yang et al. (2017) and Zhao and Yang (2019) studied the distribution characteristics of water seepage pressure in the grout region. Hai et al. (2017) and Guo et al. (2019) reveals the

CORRESPONDENCE Pengtao An apengtao@csu.edu.cn National Engineering Laboratory of High-Speed Railway Construction Technology, Central South University, Changsha 410075, China

influence of water seepage pressure by numerical simulation. Jorge et al. (2021) analyzed the source of tunnel water inflow through experiments. Xue et al. (2021) analyzed the reinforcement measures under the condition of surrounding rock through experiments. The purpose of structural safety and drainage control is realized by setting drainage pressure device (He et al., 2020).

Experts have conducted a deep analysis of prediction and treatment measures in tunnel spring water. However, the theoretical calculation assumes that the water head borne by the inner edge of the support structure is 0, resulting in a certain gap between the existing analysis formula and the actual situation (Qian and Rong, 2008; Wang et al., 2011; He et al., 2015). In the actual working condition, behind the secondary lining are the waterproof board, blind pipe and initial support. The waterproof board makes the secondary lining itself not seepage and drainage. The head pressure at the contact between the secondary lining and the initial support is extremely complex. At the same time, there is little systematic research on the calculation of the allowable drainage of parallel tunnels. Thus, first, we establish the differential equation of seepage flow in parallel tunnels and obtain the steady state funnel curve equation with seepage into the tunnel. Then, we calculate the allowable flow based on the maximum allowable decrease in groundwater at the control point and determine the descending funnel curve equation to calculate the volume of the descending funnel. In addition, the total water inflow at steady state is calculated based on the water storage coefficient. Finally, the theoretical equation is verified based on engineering examples and numerical simulation.

2. Calculation of the Allowable Tunnel Drainage

In the tunnel construction process, a large amount of groundwater will be drained by the tunnel, which will decrease the phreatic water level and damage the ecological environment. After water is pumped at a constant flow rate for a long time, a relatively stable drawdown cone is formed near the tunnel. Its shape changes with the allowable drainage volume of the tunnel.

2.1 Establishment of the Parallel Tunnel Calculation Model

When the amount of groundwater inflow into the tunnel is stable, the phreatic flow can be considered a stable flow. The phreatic flow can be considered a two-dimensional flow. A parallel tunnel drainage calculation model is established, as shown in Fig. 1.

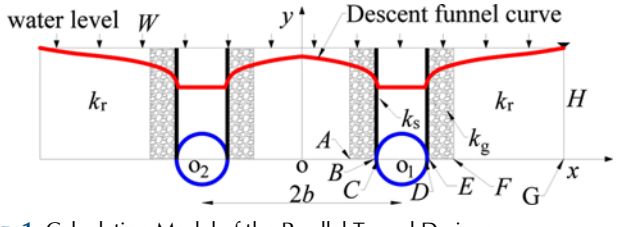

Fig. 1. Calculation Model of the Parallel Tunnel Drainage

In Fig. 1, the horizontal spacing of the parallel tunnels is $2b$; the initial water level is H; the inner and outer diameters of the initial support are r_1 and r_2, respectively; the outer edge radius of grouting reinforcement ring is a; the drainage of the parallel tunnels is 2 q; k_r, k_g and k_s are the permeabilities of the surrounding rock, grouting reinforced region and initial support, respectively; the middle of the two tunnels is section O; sections A and F are located at the outer edge of the grouting reinforced region; B and E are located at the inner edge of the grouting reinforced region; C and D are located at the inner edge of the supporting structure, and G is located at the influence radius of water inrush.

2.2 Basic Assumptions

Considering the actual situation and simplified calculation, the following assumptions are made:

1. The tunnel is located in a homogeneous and isotropic phreatic aquifer with a horizontal relative aquiclude at the bottom.
2. The upper part of the aquifer has uniform infiltration.
3. The seepage satisfies Darcy's law.
4. Parallel tunnels have equal allowable seepage values into the tunnel.
5. The source of water inflow is very sufficient.

2.3 Model Solving

When seepage is stable, the differential equation of seepage can be expressed as (Bear, 1985; Xue and Wu, 2010)

$$k\frac{\mathrm{d}}{\mathrm{d}x}\left(h\frac{\mathrm{d}h}{\mathrm{d}x}\right)+W=0\,, \tag{1}$$

where k (m/d) is the medium permeability; W (m/d) is the vertical infiltration (recharge) rate at the top of the tunnel; and h (m) is the hydraulic head at the section.

2.3.1 Solution for the Tunnel to Affect the Boundary Region

2.3.1.1 Between Regions F and G

In Fig. 1, the abscissa of sections F and G are $b+a$ (m) and $\frac{q}{W}$ (m), respectively, and the water seepage from the surrounding rock into the grouting reinforced region at section F is $q-W(a+b)$ (m^3/d/m). Then, the seepage differential equation of sections F and G is as follows:

$$\left.\begin{aligned} &k_r\frac{\mathrm{d}}{\mathrm{d}x}\left(h\frac{\mathrm{d}h}{\mathrm{d}x}\right)+W=0\\ &q-W(a+b)=k_r h\frac{\mathrm{d}h}{\mathrm{d}x}\Big|_{x\to a+b}\quad h\Big|_{x\to q/W}=H\end{aligned}\right\}. \tag{2}$$

The integral calculation result is

$$h^2=-\frac{W}{k_r}x^2+2\frac{q}{k_r}x-\frac{q^2}{k_r W}+H^2\,. \tag{3}$$

The expression of the water head in section F is

$$h_F{}^2=-\frac{W}{k_r}(a+b)^2+2\frac{q}{k_r}(a+b)-\frac{q^2}{k_r W}+H^2\,. \tag{4}$$

2.3.1.2 Between Regions E and F

The seepage quantity of section E from the grouting reinforced region to the initial support is $q - W(b + r_2)$ (m^3/d/m); then, the seepage differential equation of sections E and F is

$$\left.\begin{aligned} & k_g \frac{\mathrm{d}}{\mathrm{d}x}(h\frac{\mathrm{d}h}{\mathrm{d}x}) + W = 0 \\ & q - W(b + r_2) = k_g h \frac{\mathrm{d}h}{\mathrm{d}x}\Big|_{x \to b + r_2} \quad h\Big|_{x \to a + b} = h_F \end{aligned}\right\}. \tag{5}$$

Equation (5) is integrated to obtain Eq. (6), Eq. (4) is substituted into Eq. (6), and Eq. (7) is obtained. The hydraulic head at section E is given by Eq. (8):

$$h^2 = -\frac{W}{k_g}x^2 + 2\frac{q}{k_g}x + \frac{W(a+b)^2 - 2(a+b)q}{k_g} + h_F{}^2, \tag{6}$$

$$\begin{aligned} h^2 = & -\frac{W}{k_g}x^2 + 2\frac{q}{k_g}x + \frac{W(a+b)^2 - 2(a+b)q}{k_g} \\ & -\frac{W}{k_r}(a+b)^2 + 2\frac{q}{k_r}(a+b) - \frac{q^2}{k_r W} + H^2, \end{aligned} \tag{7}$$

$$\begin{aligned} h_E{}^2 = & \frac{W(a + r_2 + 2b)(a - r_2) - 2(a - r_2)q}{k_g} \\ & -\frac{W}{k_r}(a+b)^2 + 2\frac{q}{k_r}(a+b) - \frac{q^2}{k_r W} + H^2. \end{aligned} \tag{8}$$

2.3.1.3 Between Regions D and E

The seepage quantity of section D from the initial support into the tunnel is $q - W(b + r_1)$ (m^3/d/m); then, the seepage differential equation of sections D and E is

$$\left.\begin{aligned} & k_s \frac{\mathrm{d}}{\mathrm{d}x}(h\frac{\mathrm{d}h}{\mathrm{d}x}) + W = 0 \\ & q - W(b + r_1) = k_s h \frac{\mathrm{d}h}{\mathrm{d}x}\Big|_{x \to b + r_1} \quad h\Big|_{x \to b + r_2} = h_E \end{aligned}\right\}. \tag{9}$$

Equation (9) is integrated to obtain Eq. (10), Eq. (8) is substituted into Eq. (10), and Eq. (11) is obtained. The hydraulic head at section E is given by Eq. (12):

$$h^2 = -\frac{W}{k_s}x^2 + 2\frac{q}{k_s}x + \frac{W(b + r_2)^2 - 2(b + r_2)q}{k_s} + h_E{}^2, \tag{10}$$

$$\begin{aligned} h^2 = & -\frac{W}{k_s}x^2 + 2\frac{q}{k_s}x + \frac{W(b + r_2)^2 - 2(b + r_2)q}{k_s} \\ & + \frac{W(a + r_2 + 2b)(a - r_2) - 2(a - r_2)q}{k_g} \\ & -\frac{W}{k_r}(a+b)^2 + 2\frac{q}{k_r}(a+b) - \frac{q^2}{k_r W} + H^2, \end{aligned} \tag{11}$$

$$\begin{aligned} h_D{}^2 = & \frac{W(2b + r_1 + r_2)(r_2 - r_1) - 2(r_2 - r_1)q}{k_s} \\ & + \frac{W(a + r_2 + 2b)(a - r_2) - 2(a - r_2)q}{k_g} \\ & -\frac{W}{k_r}(a+b)^2 + 2\frac{q}{k_r}(a+b) - \frac{q^2}{k_r W} + H^2. \end{aligned} \tag{12}$$

2.3.2 Interregional Solution for the Parallel Tunnel

2.3.2.1 Between Regions O and A

Since the water inflow of the parallel tunnel is assumed to be equal when the seepage is stable, there is no horizontal seepage at section O, and the derivative of the hydraulic head is 0; the seepage volume of section A from the surrounding rock into the grouting reinforced region is $q - W(b - a)$ (m^3/d/m), and the areas of sections O and A satisfy the following expression:

$$\left.\begin{aligned} & k_r \frac{\mathrm{d}}{\mathrm{d}x}(h\frac{\mathrm{d}h}{\mathrm{d}x}) + W = 0 \\ & W(b - a) = -k_r h \frac{\mathrm{d}h}{\mathrm{d}x}\Big|_{x \to b - a} \quad 0 = \frac{\mathrm{d}h}{\mathrm{d}x}\Big|_{x \to 0} \end{aligned}\right\}. \tag{13}$$

The integral is calculated as follows:

$$h^2 = -\frac{W}{k_r}x^2 + C, \tag{14}$$

where C is a constant.

The head height at section A is

$$h_A{}^2 = -\frac{W}{k_r}(a - b)^2 + C. \tag{15}$$

2.3.2.2 Between Regions A and B

The amount of water infiltrated into the primary support from the grouting reinforced region at section B is $W(b - r_2)$ (m), and the following expression is satisfied between section A and section B:

$$\left.\begin{aligned} & k_g \frac{\mathrm{d}}{\mathrm{d}x}(h\frac{\mathrm{d}h}{\mathrm{d}x}) + W = 0 \\ & W(b - r_2) = -k_g h \frac{\mathrm{d}h}{\mathrm{d}x}\Big|_{x \to b - r_2} \quad h\Big|_{x \to b - a} = h_A \end{aligned}\right\}. \tag{16}$$

The integral is calculated as follows:

$$h^2 = -\frac{W}{k_g}x^2 + \frac{W(a-b)^2}{k_g} + h_A{}^2. \tag{17}$$

Equation (15) is substituted into Eq. (17) to obtain

$$h^2 = -\frac{W}{k_g}x^2 + \frac{W(a-b)^2}{k_g} - \frac{W}{k_r}(a-b)^2 + C. \tag{18}$$

The hydraulic head at section B is expressed as

$$h_B{}^2 = \frac{W(a - r_2)(a + r_2 - 2b)}{k_g} - \frac{W}{k_r}(a-b)^2 + C. \tag{19}$$

2.3.2.3 Between Regions B and C

The water inflow from section C is $W(b - r_1)$ (m^3/d/m), and areas B and C satisfy the following expressions:

$$\left.\begin{aligned} & k_s \frac{\mathrm{d}}{\mathrm{d}x}(h\frac{\mathrm{d}h}{\mathrm{d}x}) + W = 0 \\ & W(b - r_1) = -k_s h \frac{\mathrm{d}h}{\mathrm{d}x}\Big|_{x \to b - r_1} \quad h\Big|_{x \to b - r_2} = h_B \end{aligned}\right\}. \tag{20}$$

By integral calculation, we obtain

$$h^2 = -\frac{W}{k_s}x^2 + \frac{W(b-r_2)^2}{k_s} + h_B{}^2 . \tag{21}$$

Equation (19) is substituted into Eq. (21) and Eq. (19) is substituted into Eq. (21) and Eq. (19) is substituted into Eq. (21) and Eq. (22) is obtained. The hydraulic head at a given position is expressed as follows:

$$h^2 = -\frac{W}{k_s}x^2 + \frac{W(b-r_2)^2}{k_s} + \frac{W(a-r_2)(a+r_2-2b)}{k_g} - \frac{W}{k_r}(a-b)^2 + C, \tag{22}$$

$$h_C{}^2 = \frac{W(2b-r_1-r_2)(r_1-r_2)}{k_s} + \frac{W(a-r_2)(a+r_2-2b)}{k_g} - \frac{W}{k_r}(a-b)^2 + C. \tag{23}$$

Ignore the discretity of the tunnel seepage pressure along the support structure, assuming that $h_C = h_D$ and simultaneously solving Eqs. (12) and (23), we can determine the parameters; then, the drawdown curve with allowable tunnel discharge is obtained.

2.4 Calculation of the Total Tunnel Drainage

2.4.1 Volume Calculation of the Drawdown Funnel

Integrate the phreatic water level line to obtain

$$V = 2(H\frac{q}{W} - \int_0^{\frac{q}{W}} h dx) . \tag{24}$$

2.4.2 Calculation of the Drainage Volume

The water storage coefficient of the tunnel site area is μ^*, and the relationship between the total volume of the funnel and the total water release is

$$Q = V\mu^* . \tag{25}$$

3. Result Verification

Numerical simulation is used to test the effectiveness of the proposed method.

3.1 Parameter Determination

To validate the analytical solutions, the program FLAC^{3D} was used to establish a three-dimensional model. At present, conformal transformation is generally used to map noncircular tunnel sections to circles (Simha, 1998). The radius of the circumscribed circle of the tunnel section is taken as the equivalent circle radius (Yan et al., 2005).

$$r_{0i} = \frac{\sqrt{4h_i^2 + b_i^2}}{4\left|\cos\tan^{-1}(\frac{b_i}{2h_i})\right|} , \tag{26}$$

where r_{0i} is the tunnel radius; b_i is the tunnel span; h_i is the tunnel height.

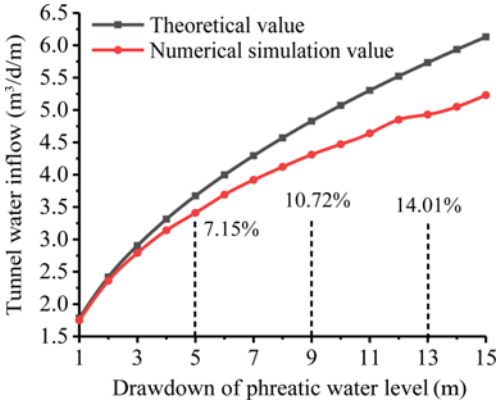

Fig. 2. Comparison of Results

3.2 Element Simulation and Boundary Conditions

Each structure is a solid unit. The normal displacement at the bottom and around is 0. Surface water can flow freely.

3.3 Analysis of Calculation Results

The calculated values of the two methods are shown in Fig. 2.

Figure 2 shows that the calculation results of the two methods are similar. The difference between them increases with the increase of phreatic water level drawdown. It shows that the formula derived in this paper is more suitable for the condition of small phreatic water level drawdown.

4. Case Study

4.1 Engineering Background

Hongtu Tunnel is located in Guangdong Province. The left and

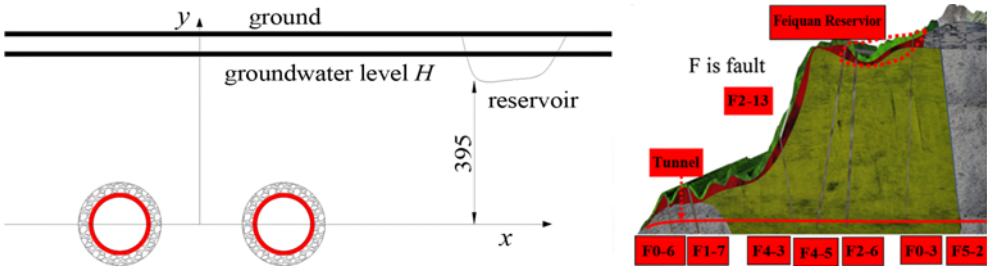

Fig. 3. Reservoir Location

right tunnels are 6,336 m and 6,337 m long, respectively, and the maximum overburden is 739 m. Through the Lianhuashan mountain range, Tongziyang syncline, Lianhuashan fault zone and Rongjiang fault zone, the outcrop rock mass on the tunnel surface is broken, the rock joints and cracks are relatively developed.

The top and bottom elevations of the reservoir dam are 720 m and 686 m, respectively, and the maximum storage capacity is approximately 25 × 10^4 m^3, as shown in Fig. 3. The designed elevation of this section of the tunnel is approximately 272 – 280 m. The precipitation infiltration intensity is 0.0035 m/d, and the water storage coefficient is 0.056. To avoid irreparable damage to the local ecological environment, the water level of the reservoir is limited to 1 m after comprehensive consider the power generation conditions and historical data of surface vegetation.

4.2 Parameter Determination

The radius of the tunnel section after the equal circle treatment is approximately 6.2 m; the thickness of primary support and secondary support is 30 cm and 50 cm respectively. The distance between the centres of the parallel tunnels is 49 m, and the stable water depth at the tunnel is 410 m.

4.3 Calculation of the Allowable Tunnel Drainage

Substitute Eq. (19) into Eq. (21) to obtain Eq. (22). The hydraulic head at a given position is expressed as follows:

$$q = Wx + \sqrt{k_r W \Delta H (2H - \Delta H)} \ . \tag{27}$$

The results show that when the reservoir drawdown is 1 m, the allowable discharge of the tunnel is 2.1 m^3/m/d.

When there is no grouting $a = r_2 = 7$ m ; according to Eq. (4), the hydraulic head of the initial support is 346.43 m, which is much greater than the maximum bearable pressure of the initial support; therefore, curtain grouting is required.

4.4 Determination of the Grouting Reinforced Region Parameters

4.4.1 Permeability of the Grouting Reinforced Region

Assuming that the head height acting on the initial support through the grouting reinforcement ring is h_E, $\alpha = \frac{h_E}{H}$, we obtain the relationship between the groundwater inflow into the tunnel and the permeability of the grouting reinforced region as follows:

$$q = W(a+b) + \frac{W(r_2 - a)}{k_g / k_r} + \frac{W}{kg / kr} \sqrt{\frac{H^2 kg^2 (1-\alpha^2) + W(k_r - k_g)(a - r_2)^2}{k_r W}} \ . \tag{28}$$

Assuming that the thickness of the grouting reinforced region is 6 m, the relationship curve between water seepage and permeability of the grouting reinforced region is shown in Fig. 4.

Figure 4 shows that when the initial support bears different seepage pressures, the water inflow of the tunnel decreases with the decrease in permeability of the grouting reinforced region.

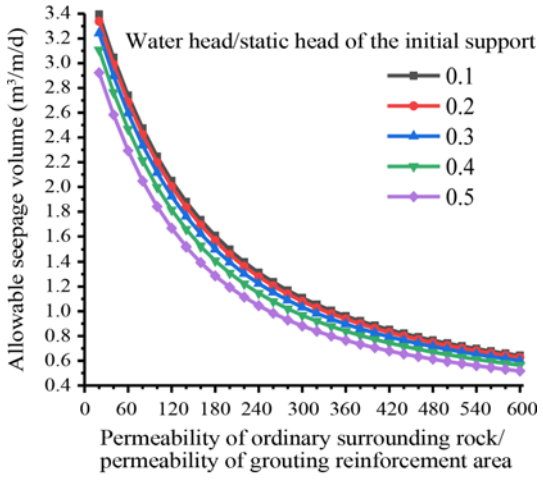

Fig. 4. Relationship between the Permeability of the Grouting Reinforced Region and the Water Inflow of the Tunnel

The g grouting reinforced region in the water-rich section can limit the drainage and ensure the stability of the tunnel during construction. However, when the permeability of the grouting reinforced region is reduced to 1/400 permeability of the surrounding rock, the grouting reinforced region has very little sensitivity to water entering the tunnel.

In addition, the head pressure of the initial support is greatly related to the amount of groundwater inflow into the tunnel. During the grouting reinforced region, the working state of the amount of groundwater inflow into the tunnel system is very important. After the drainage system has been blocked, the head pressure of the initial support will sharply increase. During the construction and operation period, the annular blind pipe should be regularly inspected to prevent damage to the tunnel structure caused by the plugging and fracturing of the initial support and secondary lining.

4.4.2 Thickness of the Grouting Reinforced Region

Considering the test section data, the permeability of surrounding

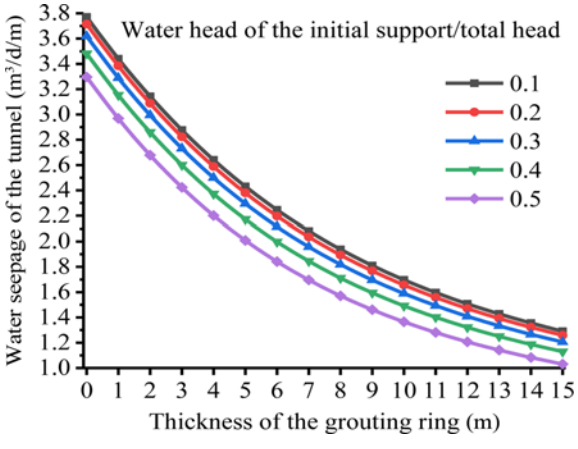

Fig. 5. Relationship between Grouting Reinforced Region and Tunnel Water Seepage

rock is 100 times that of grouting reinforcement area. Fig. 5 is a graph of influence of thickness in the grouting reinforcement region.

Figure 5 shows that the water seepage decreases with increasing grouting reinforced region, and the sensitivity decreases when the radius exceeds 10 m. Figs. 4 – 5 show that the curtain grouting reinforced region in actual working conditions is 6.0 m thick, and the reservoir depth drop and initial support head satisfy the design requirements.

The grouting reinforcing ring is a drainage structure that can be used to achieve economic and safety of its permeability and thickness. Reasonably increase its thickness and reduce its permeability, protect the support structure.

4.5 Calculation of the Total Water Inflow

The permeability of surrounding rock is 100 times and 2000 times that of grouting ring grouting and initial support respectively. Considering the complexity of the actual working conditions, the maximum water inflow is 1.5 $m^3/m/d$.

The calculation equation of the hydraulic head and falling funnel volume in each area is shown in Eqs. (29) – (30):

$$h^2=\begin{cases}-0.1522x^2+130.4348x+140149.6894 & 37.5\le x\le 428\\ -15.2174x^2+13043.4783x-322903.979 & 31.5\le x<37.5\\ -304.3478x^2+260869.5652x-7842536.044 & 31.2\le x<31.5\\ 330.0678 & 17.8\le x<31.2\\ -304.3478x^2+96759.6331 & 17.5\le x<17.8\\ -15.2174x^2+8213.4374 & 11.5\le x<17.5\\ -0.1522x^2+6221.0624 & 0\le x<11.5,\end{cases} \tag{29}$$

$$V=2(H\frac{q}{W}-\int_0^{11.5}hdx-\int_{11.5}^{17.5}hdx-\int_{17.5}^{17.8}hdx-\int_{17.8}^{31.2}hdx-\int_{31.2}^{31.5}hdx-\int_{31.5}^{37.5}hdx-\int_{37.5}^{428}hdx)=2\times(410\times\frac{1.5}{0.0035}-911-422-13-244-54-2000-160000)=24140.57\mathrm{m^3m^{-1}}. \tag{30}$$

When the seepage is stable, the falling curve is shown in Fig. 6. The calculation results of the total water inflow are as follows:

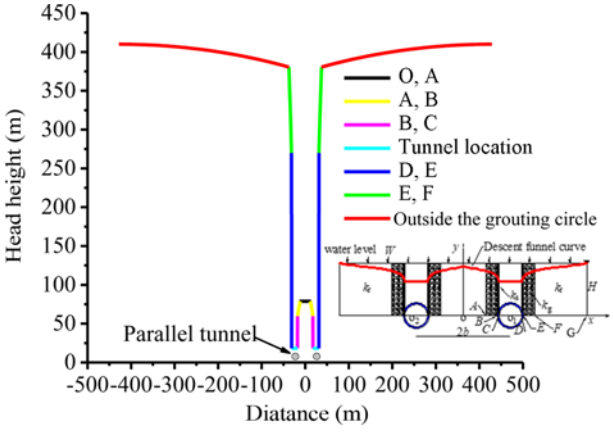

Fig. 6. Steady State Drawdown Curve

Fig. 7. Curtain Grouting Effect and Water Inflow: (a) Tunnel Face Condition after Grouting, (b) Water Inflow Measurement

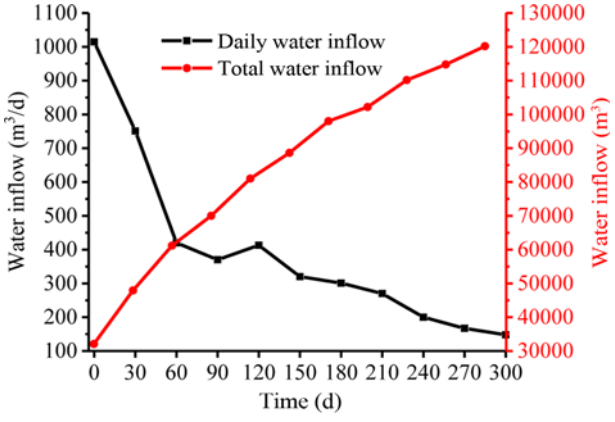

Fig. 8. Water Inflow

$$Q=V\mu^*=24140.57\times0.056=1351.87\mathrm{m^3m^{-1}}. \tag{31}$$

During the construction, advance curtain grouting was performed in this area with a total of two cycles and a length of 80 m. The total water inflow was calculated to be $1.08\times10^5\,m^3$. During nearly 9 months of the construction of the curtain grouting section, the water inflow was measured through the drainage ditch, as shown in Fig. 7, and the results are shown in Fig. 8.

The daily water inflow is basically stable after 270 days: it is 148 m^3/d, which is 18.9% different from the calculated value (1.5 × 80 = 120 m^3/d); the actual monitoring total water inflow is up to 1.2 × 10^5 m^3, which is 10% different from the theoretical calculation. The water level of the reservoir is greatly affected by weather, but the maximum drawdown is within 1 m.

To further test the effect of curtain grouting, sensor elements are embedded at the construction site, as shown in Fig. 10.

Figure 10 shows that the head head is 16 m in the initial support structure, the head height calculated by Eq. (12) is 18.17 m, and the error is 13.6%.

Based on this analysis, the calculated allowable discharge, total water inflow and height of the initial support water head are consistent with the actual conditions. The difference may be caused by the discreteness of the permeability and storage coefficient

Fig. 9. Embedding and Measurement of the Seepage Pressure

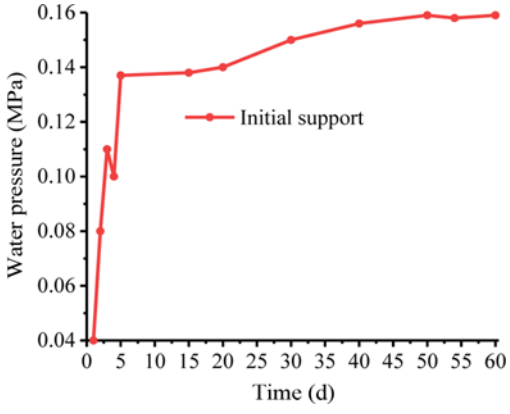

Fig. 10. Water Pressure Monitoring

and the substitution of the equivalent circle approximation. In addition, the actual water inflow values of parallel tunnels are not completely equal, which affects the calculation accuracy.

5. Conclusions

To determine the reasonable allowable drainage of parallel tunnels, a steady-flow calculation model of tunnel drainage is established. the calculation equations of the allowable drainage and total drainage when seepage reaches a steady state are derived. The main conclusions are as follows

1. The allowable drainage of the tunnel is related to the rainfall infiltration intensity, permeability of the surrounding rock, distance between the control point and the tunnel and allowable drawdown, but it is not related to the setting of the grouting reinforced region.
2. The application of a grouting reinforced region can reduce the water head pressure of the initial support and make its design more reasonable and economic.
3. The head pressure borne by the initial support has a substantial relationship with the amount of groundwater inflow into the tunnel. The circumferential blind pipe should be regularly inspected to prevent plugging and fracturing of the initial support and secondary lining, which will damage the tunnel structure.
4. Compared with the numerical simulation results, the calculation method in this paper has high accuracy when the phreatic water level drops relatively small.

Acknowledgments

This paper is jointly funded by the National Natural Science Foundation (51978668) and the Provincial Natural Science Foundation (DFH (201904) ys1-001). The authors want to acknowledge these financial assistances.

ORCID

Pengtao An https://orcid.org/0000-0002-3740-1778

References

Bear J (1985) Ground water mechanic. Geologic Publishing Company, Beijing, China, 25-123

Cheng WC, Bai XD, Sheil BB, Li G, Wang F (2020) Identifying characteristics of pipejacking parameters to assess geological conditions using optimisation algorithm-based support vector machines. *Tunnelling and Underground Space Technology* 106:103592, DOI: 10.1016/j.tust.2020.103592

Cheng P, Zhao L, Li Q, Li L, Zhang SY (2019a) Water inflow prediction and grouting design for tunnel considering nonlinear hydraulic conductivity. *KSCE Journal of Civil Engineering* 23(9):4132-4140, DOI: 10.1007/s12205-019-0306-9

Cheng P, Zhao L, Luo Z, Li L, Li Q, Deng X, Peng WQ (2019b) Analytical solution for the limiting drainage of a mountain tunnel based on area-well theory. *Tunnelling and Underground Space Technology* 84:22-30, DOI: 10.1016/j.tust.2018.10.014

Fu HL, An PT, Chen L, Cheng GW (2022) Impact of water gushing influenced by the relationship between fault and tunnel position. *Journal of Performance of Constructed Facilities* 36(1), DOI: 10.1061/(ASCE)CF.1943-5509.0001681

Gokdemir C, Rubin Y, Li XJ, Li YD, Xu H (2019) Vulnerability analysis method of vegetation due to groundwater table drawdown induced by tunnel drainage. *Advances in Water Resources* 133:103406, DOI: 10.1016/j.advwatres.2019.103406

Guo HY, Ji YY, Fang L, Li K, Tang CP, Wang SF (2019) External water pressures and limited emission standards of water-rich tunnels based on fluid-solid coupling analysis. *Chinese Journal of Geotechnical Engineering* 41(S1):165-168 (in Chinese)

Hai S, Mingzhou B, Shaochuan X (2017) Mechanics parameter

optimization and evaluation of curtain grouting material in deep, water-rich karst tunnels. *Advances in Materials Science and Engineering* 2017, DOI: 10.1155/2017/1853951

He BG, Li H, Zhang XW, Xie JH (2020) A novel analytical method incorporating valve pressure for the controlled drainage of transport tunnels. *Tunnelling and Underground Space Technology* 106:103637, DOI: 10.1016/j.tust.2020.103637

He BG, Zhang ZQ, Fu SJ, Liu ZJ (2015) An analytical solution of water loading on tunnel supporting system with drainage of blind tube and isolation effect of waterproof board. *Chinese Journal of Rock Mechanics and Engineering* 34(S2):3936-3947 (in Chinese)

Jorge H, Marisol M, Emilio C (2021) Deciphering the origin of groundwater inflow into the Talave tunnel (SE Spain). *Science of the Total Environment* 789:147904, DOI: 10.1016/j.scitotenv.2021.147904

Kolymbas D, Wagner P (2007) Groundwater ingress totunnels - The exact analytical solution. *Tunnelling and Underground Space Technology* 22(1): 23-27, DOI: 10.1016/j.tust.2006.02.001

Li Z, He C, Ding JJ, Yang SZ (2017) A method to predict the relationship between water discharge and pressure during operational period of city tunnels constructed using the mining method. *Engineering Mechanics* 34(1):14-21 (in Chinese)

Li J, Mo HQ (2020) Study on seepage into arbitrary shape tunnel considering grouting ring. *Journal of Railway Science and Engineering* 17(5): 1228-1234, DOI: 10.19713/j.cnki.43-1423/u.T20190706 (in Chinese)

Nilsen B (2014) Characteristics of water ingress in Norwegian subsea tunnels. *Rock Mechanics and Rock Engineering* 47(3):933-945, DOI: 10.1007/s00603-012-0300-8

Park KH, Lee JG, Owatsiriwong A (2008) Seepage force in a drained circular tunnel: An analytical approach. *Canadian Geotechnical Journal* 45(3):432-436, DOI: 10.1139/T07-113

Qian QH, Rong XL (2008) State, issues and relevant recommendations for security risk management of China's underground engineering. *Chinese Journal of Rock Mechanics and Engineering* 27(4):649-655, DOI: 10.3321/j.issn:1000-6915.2008.04.001 (in Chinese)

Sembenelli PG, Sembenelli G (1999) Deep jet-grouted cut-offs in riverine alluvia for ertan cofferdams. *Journal of Geotechnical and Geoenvironmental Engineering* 125(2):142-153

Simha KRY, Mohapatra SS (1998) Stress concentration around irregular holes using complex variable method. *Sadhana* 23(4):393-412, DOI: 10.1007/BF02745750

Tao XL, Ma JR, Zeng W (2015) Treatment effect investigation of underground continuous impervious curtain application in water-rich strata. *International Journal of Mining Science and Technology* 25(6):975-981, DOI: 10.1016/j.ijmst.2015.09.015

Wang Q, Qu LQ, Guo HY, Wang QS (2011) Grouting reinforcement technique of Qingdao Jiaozhou bay subsea tunnel. *Chinese Journal of Rock Mechanics and Engineering* 30(4):790-802 (in Chinese)

Xue ZF, Cheng WC, Wang L, Song GY (2021) Improvement of the shearing behaviour of loess using recycled straw fiber reinforcement. *KSCE Journal of Civil Engineering* 25(9):3319-3335, DOI: 10.1007/s12205-021-2263-3

Xue YQ, Wu JC (2010) Groundwater dynamics (the third edition). Geological Publishing House, Beijing, China, 18-39 (in Chinese)

Yan CL, Ding DX, Bi ZW, Cui ZD (2005) Viscoelastic mechanical analysis of the stability of surrounding rock in deep tunnels. *Journal of Guizhou University of Technology (Natural Science Edition)* 34(3):125-129 (in Chinese)

Yang SZ, He C, Li Z, Yang WB, Luo YW (2017) Inner water pressure distribution law of the tunnel grouting circle in water-rich area. *Journal of China University of Mining and Technology* 46(3):546-553 (in Chinese)

Yang FR, Lee CH, Kung WJ, Yeh HF (2009) The impact of tunneling construction on the hydrogeological environment of "Tseng-Wen Reservoir Transbasin Diversion Project" in Taiwan. *Engineering Geology* 103(1-2):39-58, DOI: 10.1016/j.enggeo.2008.07.012

Zhang DL, Sun ZY (2019) An active control waterproof and drainage system of subsea tunnels and its design method. *Chinese Journal of Rock Mechanics and Engineering* 38(1):1-17 (in Chinese)

Zhao X, Yang X (2019) Experimental study on water inflow characteristics of tunnel in the fault fracture zone. *Arabian Journal of Geosciences* 12(13):399, DOI: 10.1007/s12517-019-4561-3